Open

ORIGINAL ARTICLE

Reversal in competitive dominance of a toxic versus non-toxic cyanobacterium in response to rising CO$_2$

Dedmer B Van de Waal[1,2,4], Jolanda MH Verspagen[1], Jan F Finke[1,5], Vasiliki Vournazou[1], Anne K Immers[1,2], W Edwin A Kardinaal[1,6], Linda Tonk[1,7], Sven Becker[2,8], Ellen Van Donk[2,3], Petra M Visser[1] and Jef Huisman[1]

[1]Department of Aquatic Microbiology, Institute for Biodiversity and Ecosystem Dynamics, University of Amsterdam, Amsterdam, The Netherlands; [2]Department of Aquatic Ecology, Netherlands Institute of Ecology, Wageningen, The Netherlands and [3]Department of Palaeoecology, Institute of Environmental Biology, University of Utrecht, Utrecht, The Netherlands

Climate change scenarios predict a doubling of the atmospheric CO$_2$ concentration by the end of this century. Yet, how rising CO$_2$ will affect the species composition of aquatic microbial communities is still largely an open question. In this study, we develop a resource competition model to investigate competition for dissolved inorganic carbon in dense algal blooms. The model predicts how dynamic changes in carbon chemistry, pH and light conditions during bloom development feed back on competing phytoplankton species. We test the model predictions in chemostat experiments with monocultures and mixtures of a toxic and non-toxic strain of the freshwater cyanobacterium *Microcystis aeruginosa*. The toxic strain was able to reduce dissolved CO$_2$ to lower concentrations than the non-toxic strain, and became dominant in competition at low CO$_2$ levels. Conversely, the non-toxic strain could grow at lower light levels, and became dominant in competition at high CO$_2$ levels but low light availability. The model captured the observed reversal in competitive dominance, and was quantitatively in good agreement with the results of the competition experiments. To assess whether microcystins might have a role in this reversal of competitive dominance, we performed further competition experiments with the wild-type strain *M. aeruginosa* PCC 7806 and its *mcyB* mutant impaired in microcystin production. The microcystin-producing wild type had a strong selective advantage at low CO$_2$ levels but not at high CO$_2$ levels. Our results thus demonstrate both in theory and experiment that rising CO$_2$ levels can alter the community composition and toxicity of harmful algal blooms.
The ISME Journal (2011) 5, 1438–1450; doi:10.1038/ismej.2011.28; published online 10 March 2011
Subject Category: microbial population and community ecology
Keywords: competition model; harmful cyanobacteria; inorganic carbon; microcystin; *Microcystis aeruginosa*; resource competition

Introduction

Climate change scenarios predict that atmospheric CO$_2$ concentrations will rise to ∼750 p.p.m. by the year 2100 (Solomon *et al.*, 2007). This may have

Correspondence: J Huisman, Department of Aquatic Microbiology, Institute for Biodiversity and Ecosystem Dynamics, University of Amsterdam, PO Box 94248, Amsterdam 1090 GE, The Netherlands.
E-mail: j.huisman@uva.nl
[4]Present address: Alfred Wegener Institute for Polar and Marine Research, Am Handelshafen 12, 27570 Bremerhaven, Germany.
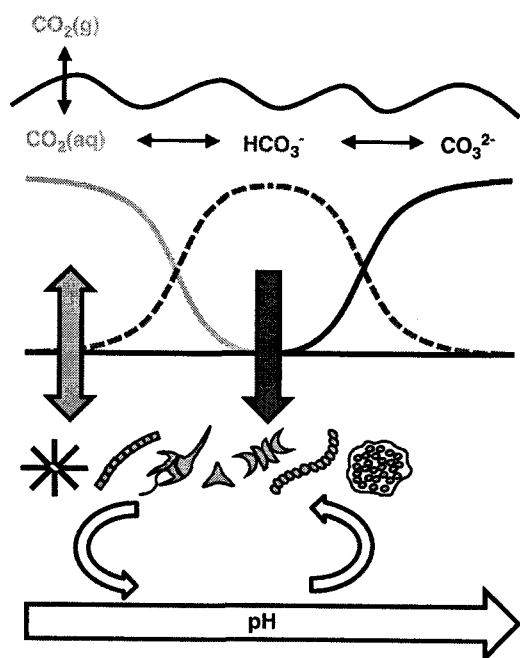[5]Present address: Department of Earth and Ocean Sciences, University of British Columbia, 6339 Stores Road, Vancouver, British Columbia, Canada.
[6]Present address: KWR Watercycle Research Institute, Groningenhaven 7, 3433 PE Nieuwegein, The Netherlands.
[7]Present address: Global Change Institute, University of Queensland, St Lucia, Qld 4072, Australia.
[8]Present address: Biodiversity Institute of Ontario, University of Guelph, Guelph, Ontario, Canada.

considerable impact on aquatic microbial communities. Cyanobacteria and eukaryotic phytoplankton utilize CO$_2$ for photosynthesis, and account for almost 50% of the carbon fixation of the world (Field *et al.*, 1998; Behrenfeld *et al.*, 2006). Yet, theory capable of predicting how rising CO$_2$ will affect the species composition of these communities is still in its infancy.

Resource competition theory aims to predict changes in species composition (Tilman, 1982; Grover, 1997). Mathematical models have been developed that link the population dynamics of competing species with dynamic changes in resource availability. Competition experiments can be run to test the theory, providing a check on the validity of the models or suggesting new directions for research. Competition for nutrients such as nitrogen and phosphorus has been extensively studied in this way (Tilman, 1982; Sommer, 1985; Ducobu *et al.*, 1998; Klausmeier *et al.*, 2004). Competition for light has also been well investigated

Figure 1 Conceptual diagram of the main biological and chemical interactions involved in competition for inorganic carbon.

(Huisman et al., 1999; Litchman and Klausmeier, 2001; Stomp et al., 2004; Passarge et al., 2006). However, with a few exceptions (Williams and Turpin, 1987; Caraco and Miller, 1998), competition for inorganic carbon has not been addressed.

The major challenge here is that competition for inorganic carbon is conceptually and experimentally more complex than competition for other limiting resources (Figure 1). Dissolved CO_2 reacts with water, and subsequently dissociates into bicarbonate and a proton. Hence, rising concentrations of dissolved CO_2 cause a reduction in pH, a phenomenon known as ocean acidification (Orr et al., 2005; Riebesell et al., 2007; Doney et al., 2009). CO_2 uptake for photosynthesis reverses this chemical reaction. High photosynthetic rates can deplete the dissolved CO_2 concentration (Hein, 1997; Ibelings and Maberly, 1998), thereby inducing high pH (Talling, 1976; Maberly, 1996; Hansen, 2002). Changes in pH shift the speciation of dissolved inorganic carbon, from CO_2 at low pH to bicarbonate at intermediate pH and carbonate at high pH (Figure 1). Although phytoplankton species cannot use carbonate as carbon source, many species can take up both CO_2 and bicarbonate (Kaplan and Reinhold, 1999; Martin and Tortell, 2008). However, major species-specific differences exist in relative uptake rates of these two carbon sources (for example, Rost et al., 2003; Price et al., 2008; Maberly et al., 2009), which may affect their competitive interactions (Raven, 1991; Tortell et al., 2002; Rost et al., 2008). Thus, competition for CO_2 involves depletion of the limiting resource (inorganic carbon), a shift in the relative availability

of different inorganic carbon sources (CO_2 versus bicarbonate), and a shift in associated environmental conditions (pH).

Competition for inorganic carbon may be particularly relevant in dense algal blooms of eutrophic waters. The high photosynthetic activity of dense algal blooms can strip the surface layer from dissolved inorganic carbon, thereby inducing high pH and carbon-limited growth conditions (Hein, 1997; Ibelings and Maberly, 1998). However, rising atmospheric CO_2 concentrations will enrich surface blooms with inorganic carbon, such that their growth may become limited by other factors. In particular, dense algal blooms also increase the turbidity of the water, thus reducing light availability as a result of self-shading (Huisman et al., 1999, 2004). Hence, competitive interactions within dense blooms might shift from competition for inorganic carbon under low CO_2 conditions to competition for light in a high CO_2 world.

In this paper, we develop a new theory to predict how species compete for inorganic carbon and light. The theory will focus on dynamic changes in carbon chemistry, pH and light conditions during bloom development, and how these environmental changes feed back on the competing species. The theory is tested in chemostat experiments, with full control of CO_2, temperature, light and nutrient conditions. The experiments are carried out with a toxic and non-toxic strain of the freshwater cyanobacterium *Microcystis aeruginosa*, which is a cosmopolitan species causing harmful algal blooms in many eutrophic waters (Chen et al., 2003; Rinta-Kanto et al., 2005; Verspagen et al., 2006; Paerl and Huisman, 2008).

Theory

We develop a model that considers several phytoplankton species competing for inorganic carbon and light in a dense algal bloom. In this section, we explain the model structure and key assumptions; the full model is presented in the Supplementary Information. The model assumes that all nutrients are in ample supply, such that the specific growth rates of the competing species depend on their intracellular carbon content (Droop, 1973; Grover, 1991a). Let X_i denote the population density of species i, and let Q_i denote its cellular carbon content. The population dynamics of n competing species can then be summarized by two sets of differential equations:

$$\frac{dX_i}{dt} = \mu_{max,i}\left(\frac{Q_i - Q_{min,i}}{Q_{max,i} - Q_{min,i}}\right)X_i - m_iX_i \quad (1)$$

$i = 1, \ldots, n$

$$\frac{dQ_i}{dt} = u_{CO_2,i} + u_{HCO_3^-,i} - r_i - \mu_iQ_i \quad (2)$$

$i = 1, \ldots, n$

The first set of equations describes the population densities of the competing species, where $\mu_{max,i}$ is the maximum specific growth rate of species i, $Q_{min,i}$ is its minimum cellular carbon content required for growth, $Q_{max,i}$ is its maximum cellular carbon content, and m_i is its specific loss rate. The second set of equations describes the cellular carbon contents of the species, which increase through uptake of carbon dioxide ($u_{CO_2,i}$) and bicarbonate ($u_{HCO_3,i}$), and decrease through respiration (r_i) and through dilution of cellular carbon by growth. We assume that uptake rates of carbon dioxide and bicarbonate are increasing but saturating functions of ambient CO_2 and bicarbonate concentrations, as in Michaelis–Menten kinetics, and are suppressed when cells become satiated with carbon (Morel, 1987; Ducobu et al., 1998). As carbon assimilation requires energy, we further assume that these uptake rates depend on photosynthetic activity and hence on light availability.

Carbon dioxide dissolves in water, and may subsequently dissociate into bicarbonate and a proton. This dissociation depends on pH and is relatively slow (Stumm and Morgan, 1996). Bicarbonate can dissociate further into carbonate and a proton. This is a much faster process, that is essentially in equilibrium with alkalinity and pH (Stumm and Morgan, 1996). Therefore, let [CO_2] denote the total concentration of dissolved carbon dioxide (including carbonic acid), and let [CARB] denote the total concentration of bicarbonate and carbonate. The total dissolved inorganic carbon is $DIC = [CO_2] + [CARB]$. Changes in dissolved inorganic carbon can then be described by (Johnson, 1982; Stumm and Morgan, 1996):

$$\frac{d[CO_2]}{dt} = D([CO_2]_{in} - [CO_2]) + g_{CO_2} + c_{CO_2}$$
$$+ \sum_{i=1}^{n} r_i X_i - \sum_{i=1}^{n} u_{CO_2,i} X_i \tag{3}$$

$$\frac{d[CARB]}{dt} = D([CARB]_{in} - [CARB]) - c_{CO_2}$$
$$- \sum_{i=1}^{n} u_{HCO_3^-,i} X_i \tag{4}$$

The first equation describes changes in the concentration of dissolved carbon dioxide through the influx ([CO_2]$_{in}$) and efflux of water containing dissolved CO_2, through gas exchange with atmospheric CO_2 (g_{CO_2}), and through the chemical reaction from dissolved CO_2 to bicarbonate and vice versa (c_{CO_2}). In addition, the concentration of dissolved carbon dioxide increases through respiration (r_i) and decreases through uptake of CO_2 ($u_{CO_2,i}$) by the species. The second equation describes changes in the summed concentration of bicarbonate and carbonate through in- and efflux of water containing these inorganic carbon species, through

the chemical reaction from bicarbonate to dissolved CO_2 and vice versa (c_{CO_2}), and through uptake of bicarbonate ($u_{HCO_3,i}$) by the species. Concentrations of bicarbonate and carbonate were calculated from [CARB] assuming equilibrium with alkalinity and pH (Stumm and Morgan, 1996; see Supplementary Information for details).

Materials and methods

Species
The model was tested using a toxic and non-toxic strain of the freshwater cyanobacterium M. aeruginosa (Kützing) Kützing. The toxic strain Microcystis CYA140 produces the hepatotoxin microcystin-LR, whereas the non-toxic strain Microcystis CYA43 does not produce microcystins (Van der Grinten et al., 2000). Both strains were obtained from the Norwegian Institute for Water Research, and have been used in many laboratory studies as common representatives of toxic versus non-toxic Microcystis strains. They were grown as single cells and not in colonies. The monoculture experiments were unialgal but not axenic. However, regular microscopic inspection confirmed that abundances of heterotrophic bacteria remained low (that is, <1% of the total biomass) for the entire duration of the experiments.

Chemostat experiments
All experiments were carried out in chemostats specifically designed to study competition among phototrophic microorganisms (Huisman et al., 1999; Stomp et al., 2004; Passarge et al., 2006). Each chemostat consisted of a flat culture vessel illuminated from one side to obtain a unidirectional light gradient. Light was supplied at constant incident irradiance I_{in} using white fluorescent tubes (Philips PL-L 24W/840/4P, Philips Lighting, Eindhoven, The Netherlands). The chemostats had an optical path length (mixing depth) of $z_m = 5$ cm, and an effective working volume of 1.7 l. The chemostats were run at a dilution rate of $D = 0.011$ h^{-1}, and maintained at a constant temperature of 21.5 ± 1 °C using a metal cooling finger connected to a Colora thermocryostat. The chemostats were supplied with a nutrient-rich mineral medium as described by Van de Waal et al. (2009) to prevent nutrient limitation during the experiments. The mineral medium had a pH of ~ 8.2 in the absence of cyanobacteria. The chemostats were aerated with moistened and sterilized (0.2 µm Millex-FG Vent Filter, Millipore, Billerica, MA, USA) N$_2$ gas enriched with CO_2 to a final gas flow of 25 l h^{-1} using Brooks Mass Flow Controllers (Brooks Instrument, Hatfield, PA, USA). The gas was moistened with milli-Q water to suppress evaporation of water from the chemostats by the continuous gas flow.

To obtain carbon-limited conditions, we supplied the chemostats with a low partial pressure of

$pCO_2 = 200$ p.p.m. in the gas flow, a low bicarbonate concentration of $500 \, \mu mol \, l^{-1}$ $NaHCO_3$, and an incident light intensity of $I_{in} = 50 \pm 1 \, \mu mol$ photons $m^{-2} \, s^{-1}$. At the onset of the competition experiment, we inoculated the two strains at a 50:50 ratio in terms of cell numbers (corresponding to a 28:72 ratio in terms of the biovolumes of the toxic versus non-toxic strain, as cells of the toxic strain were smaller).

Experimental data under light-limited conditions were obtained from Kardinaal et al. (2007b). They ran monoculture and competition experiments with the same toxic and non-toxic Microcystis strains CYA140 and CYA43 using the same experimental set-up as in our experiments. However, to obtain light-limited conditions, they used a higher partial pressure of $pCO_2 = 1000$ to 1250 p.p.m. in the gas flow, a higher bicarbonate concentration of $2000 \, \mu mol \, l^{-1}$ $NaHCO_3$ and a lower incident light intensity of $I_{in} = 25 \pm 1 \, \mu mol$ photons $m^{-2} \, s^{-1}$. In their competition experiment, the toxic versus non-toxic strain were inoculated at a 90:10 ratio in terms of biovolume, thus giving the toxic strain an initial advantage. The experimental settings are summarized in Table 1.

Population densities, light, carbon and nutrients
During the experiments, several variables were measured every other day. The incident irradiance (I_{in}) and the irradiance penetrating through the chemostat vessel (I_{out}) were measured with a LI-COR LI-250 quantum photometer (LI-COR Biosciences, Lincoln, NE, USA) at 10 randomly chosen positions on the front and back surface of the chemostat vessel, respectively. Cell numbers and biovolumes of Microcystis were determined in triplicate using a Casy 1 TTC cell counter with a 60 μm capillary (Schärfe System GmbH, Reutlingen, Germany). Because the two strains differed in average cell size, and cell size of the non-toxic strain was affected by the experimental treatments, we expressed population densities in terms of biovolume.

DIC concentrations in the chemostats were determined by sampling 15 ml of culture suspension, which was gently filtered over 0.45 μm membrane filters at low pressure (Whatman, Maidstone, UK). DIC was analyzed by a Model 700 TOC Analyzer (OI Corporation, College Station, TX, USA). The concentration of dissolved CO_2 and bicarbonate in the chemostat vessels was calculated from total DIC, pH and temperature (Stumm and Morgan, 1996). The pH was measured with a SCHOTT pH meter (SCHOTT AG, Mainz, Germany). Alkalinity was determined in a 50 ml sample that was titrated in 0.1–1 ml steps with $0.01 \, mol \, l^{-1}$ HCl to a pH of 3.0. The alkalinity was subsequently calculated using Gran plots according to Stumm and Morgan (1996).

Intracellular carbon, nitrogen, sulfur and phosphorus content were sampled in triplicate. Samples were pressurized at 10 bar to collapse the gas vesicles of Microcystis and subsequently centrifuged for 15 min at $2000 \, g$. After discarding the supernatant, the pellet was resuspended in demineralized water and centrifuged for 5 min at $15\,000 \, g$. The supernatant was discarded, pellets were stored at $-20 \, °C$ and subsequently freeze dried and weighted to determine dry weight. The carbon, nitrogen and sulfur contents of homogenized freeze-dried cell powder were analyzed using a Vario EL Elemental Analyzer (Elementar Analysensysteme GmbH, Hanau, Germany). To determine the phosphorus content, cells were oxidized with potassium persulfate for 1 h at $100 \, °C$ (Wetzel and Likens, 2000), and phosphorus concentrations were subsequently analyzed colorimetrically according to Murphy and Riley (1962).

Quantitative PCR
The toxic and non-toxic Microcystis strain looked very similar, and could not be distinguished by means of light microscopy, cell counters or flow cytometry. Therefore, we used quantitative real-time PCR (qPCR) to quantify the population densities of the toxic and non-toxic strain in the competition experiments (Kurmayer and Kutzenberger, 2003; Vaitomaa et al., 2003; Rinta-Kanto et al., 2005). This improves earlier methodology developed by

Table 1 System parameters used in the chemostat experiments

Parameter	Description	Carbon-limited chemostats	Light-limited chemostats	Units
D	Dilution rate	0.011	0.011	h^{-1}
I_{in}	Incident irradiance	50	25	μmol photons $m^{-2} \, s^{-1}$
z_m	Mixing depth	0.05	0.05	m
K_{bg}	Background turbidity[a]	8 to 12.5	4 to 9	m^{-1}
T	Temperature	21.5	21.5	°C
a	Gas flow rate	25	25	$l \, h^{-1}$
γ	Constant of proportionality for gas influx[a]	1.4×10^{-4} to 2.0×10^{-4}	1.4×10^{-4} to 2.0×10^{-4}	l^{-1}
$pCO2$	Partial pressure of CO2 in gas inflow	200	1000 to 1250	p.p.m.
$[CO_2]_{in}$	Concentration of dissolved CO2 at influx	8	29	$\mu mol \, l^{-1}$
$[CARB]_{in}$	Summed concentration of bicarbonate and carbonate at influx	500	2000	$\mu mol \, l^{-1}$
ALK_{in}	Alkalinity at influx	0.80	2.1	$mEq \, l^{-1}$

[a]Background turbidity and the constant of proportionality for gas influx had different values for different chemostat vessels.

Kardinaal et al. (2007b), who distinguished the same two strains with a less precise semiquantitative method using denaturing gradient gel electrophoresis. We extracted the DNA of all cells and measured the copy numbers of the mcyE region of the microcystin synthetase gene cluster in comparison with the copy numbers of the 16S rDNA gene (16S). The mcyE gene is present only in the toxic strain CYA140, whereas the 16S gene is present in both strains. The mcyE:16S ratios were normalized to the known inoculation ratio of the two strains at the onset of the competition experiment. Thus, the normalized mcyE:16S ratio indicates the relative abundance of the toxic strain in the total Microcystis population, where the total Microcystis population was counted by the Casy 1 TTC cell counter as described earlier.

The mcyE gene was amplified using the Maeru-mcyEF (5′-CCCTAGCATCGGGTTATCAT-3′) and Maeru-mcyER (5′-CGAGTCAATTGATATTCAATTTCTC-3′) primers (modified from Rantala et al., 2004), and the 16S rDNA gene was amplified using the Maeru-16SrDNAF (5′-GCGTGCTACTGGGCTGTA-3′) and Maeru-16SrDNAR (5′-TCGGGTCGATACAAGCC-3′) primers (modified from Doblin et al., 2007).

Aliquots of culture suspension were pressurized at 10 bar to collapse the gas vesicles of Microcystis cells, and subsequently centrifuged for 5 min at 15 000 g. After removal of supernatant, genomic DNA was extracted using a DNeasy Blood & Tissue Kit according to the manufacturer's instruction (Qiagen GmbH, Hilden, Germany). The DNA concentration of the samples was measured using a NanoDrop ND-1000 (Nano-Drop Technologies, Wilmington, DE, USA), and all samples were diluted to an equal density of $10 \, ng \, \mu l^{-1}$. The qPCR was performed with a Rotor Gene 6000 thermal cycling system (Corbett Research, Sydney, Australia). Each reaction was performed in triplicate. The reaction mix contained $2 \, \mu l$ of sample DNA in combination with $10 \, \mu l$ ABSolute QPCR SYBR green mix (ABgene, Epsom, UK), $0.3 \, \mu l$ of both the forward and reversed primer of the specific gene tested for, and was filled with $0.1 \, \mu m$ filter sterilized DNase-, RNase- and Protease-free water (Sigma-Aldrich, St Louis, MO, USA) to reach a final reaction volume of $20 \, \mu l$. The thermal cycle consisted of an initial denaturation at 95 °C for 15 min, followed by 40 cycles of denaturation at 94 °C for 20 s, and annealing for 60 s at 65 °C. Data were acquired at 65 °C, and reaction products were verified by DNA melting curve analysis at a temperature ranging from 60 °C to 95 °C at steps of 0.5 °C. Amplification efficiencies of qPCR reactions were similar in all experiments (data not shown).

Microcystin analysis
According to expectation, the microcystin concentration in the competition experiments should vary with the population density of the toxic strain. The performance of the qPCR analysis could therefore be assessed independently, by comparison of the estimated population densities of the toxic strain against the total microcystin concentration measured in the culture vessel.

Intracellular microcystin content was determined in triplicate by sampling 5–20 ml of culture suspension, which was immediately filtered using Whatman GF/C filters (pore size $\sim 1.2 \, \mu m$). Filters were frozen at −20 °C and subsequently freeze dried. Microcystins were extracted in three rounds with 75% MeOH according to Fastner et al. (1998), with an additional step for grinding of the filters using a Mini Beadbeater (BioSpec Products, Bartlesville, OK, USA) with 0.5 mm silica beads (Tonk et al., 2005). Dried extracts were stored at −20 °C and dissolved in 50% MeOH for microcystin analysis using high-performance liquid chromatography with photodiode array detection (Kontron Instruments, Watford, UK). The different microcystin variants were separated using a LiChrospher 100 ODS $5 \, \mu m$ LiChorCART 250-4 cartridge system (Merck, Darmstadt, Germany) and a 30–70% acetonitrile gradient in milli-Q water with 0.05% trifluoroacetic acid at a flow rate of $1 \, ml \, min^{-1}$. Identification of the different microcystin variants was based on their characteristic ultraviolet spectra (Lawton et al., 1994). This confirmed previous studies that Microcystis CYA140 produces microcystin-LR, whereas Microcystis CYA43 does not produce microcystins (for example, Van der Grinten et al., 2000). Microcystin-LR concentrations were quantified using a gravimetrical standard of microcystin-LR (provided by the University of Dundee).

Extracellular microcystin concentrations were determined in triplicate by filtration of 10 ml culture suspension using Whatman GF/C filters (pore size $\sim 1.2 \, \mu m$). Extracellular microcystin concentrations were below the detection limit of the high-performance liquid chromatography (2.5 ng microcystin). Therefore, the filtrate was analyzed using an enzyme-linked immunosorbant assay according to the manufacturer's protocol (EnviroLogix, Portland, ME, USA). This showed that extracellular microcystins comprised <2% of the total microcystin concentrations in all chemostat experiments, which was considered negligible.

Results

Carbon-limited experiments
In monoculture experiments under CO_2-limited conditions, population densities gradually increased until a steady state was reached after 20–30 days (Figures 2a and b). Light penetration through the chemostats (I_{out}) decreased with increasing population density. Steady-state values of I_{out} ranged from 5 to $12 \, \mu mol$ photons $m^{-2} \, s^{-1}$, which is well above the I_{out} values measured under light-limited but CO_2 replete conditions (see below). This
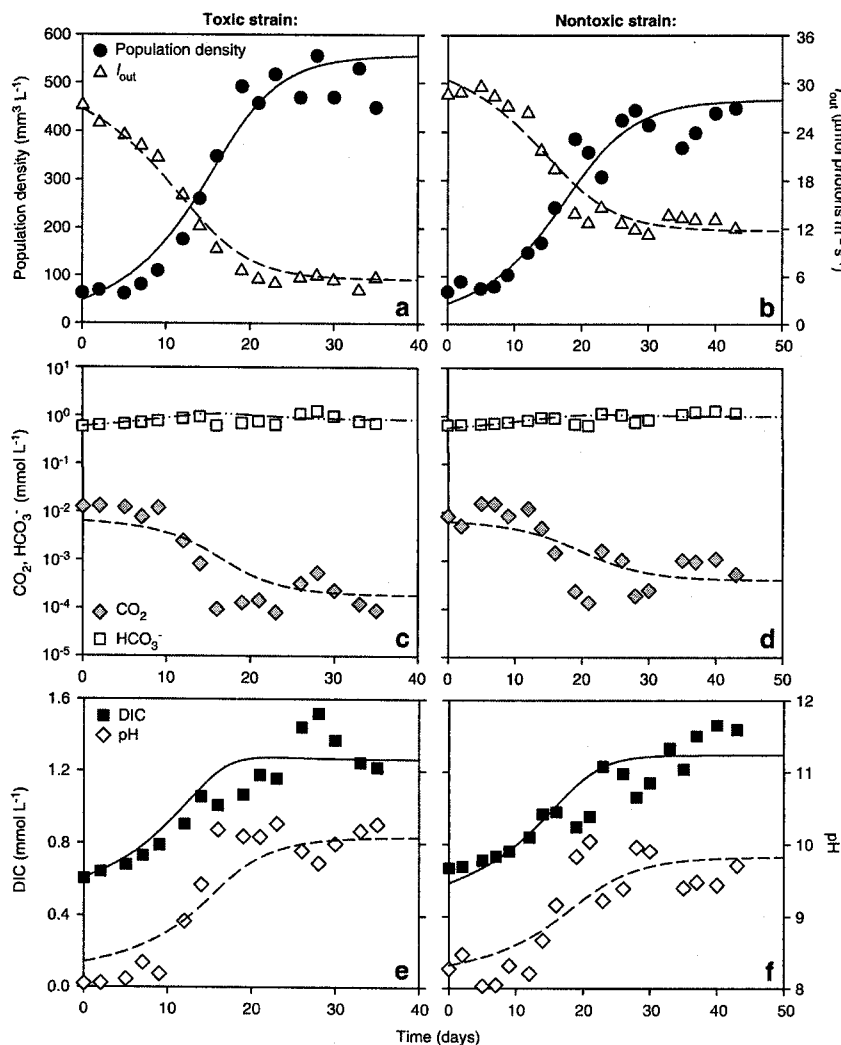
Figure 2 Monoculture experiments in CO_2-limited chemostats. (**a**, **b**) Population density (expressed as biovolume) and light intensity penetrating through the chemostat (I_{out}). (**c**, **d**) CO_2 and bicarbonate concentrations. (**e**, **f**) Dissolved inorganic carbon (DIC) and pH. Panels **a**, **c** and **e** show data for the toxic strain *Microcystis* CYA140, whereas **b**, **d** and **f** show data for the non-toxic strain *Microcystis* CYA43. Symbols represent chemostat data, lines show the model fits. Parameter values are given in Tables 1 and 2.

indicates that the steady-state chemostats were not light-limited.

As a result of increasing population densities, the carbon chemistry and pH in the water changed (Figures 2c–f). Dissolved CO_2 concentrations were rapidly depleted, showing a more than 10-fold drop to steady-state values of $\sim 0.2\, \mu mol\, l^{-1}$ in the monoculture of the toxic strain (Figure 2c) and $\sim 0.4\, \mu mol\, l^{-1}$ in the monoculture of the non-toxic strain (Figure 2d). CO_2 depletion was accompanied by an increase of pH to steady-state values of ~ 10 for the toxic strain and ~ 9.8 for the non-toxic strain (Figures 2e and f). Bicarbonate thus became the predominant carbon species in the water, comprising 65% and 77% of the total DIC in the steady-state monocultures of the toxic and non-toxic strain, respectively. The observation of strong CO_2 depletion and high pH confirms that these monoculture experiments were indeed exposed to CO_2-limited conditions.

The species parameters were estimated from the monoculture experiments, by fitting the model to the monoculture data (see Supplementary Information for methodology). This showed that the toxic strain has lower half-saturation constants for CO_2 and bicarbonate and a lower minimum carbon content than the non-toxic strain (Table 2). On the basis of these parameter estimates, the model predicts that the toxic strain should be a better competitor for CO_2 and bicarbonate than the non-toxic strain. The model predictions were tested in competition experiments. Under CO_2-limited conditions, both strains initially increased (Figure 3a). After 35 days, dissolved CO_2 was depleted to $\sim 0.2\, \mu mol\, l^{-1}$ (Figure 3b) and pH had increased to ~ 10 (Figure 3c). Hence, the non-toxic strain started to decrease and was gradually displaced by the toxic strain (Figure 3a). After 45 days, the non-toxic strain was completely excluded. The total microcystin concentration increased toward steady-state values,

Table 2 Parameter values estimated from the monoculture experiments, for the non-toxic strain *Microcystis* CYA43 and the toxic strain *Microcystis* CYA140

Parameter	Description	CYA43	CYA140	Units
μ_{max}	Maximum growth rate	0.80	0.86	Per day
m	Specific loss rate	0.264	0.264	Per day
k	Specific light attenuation coefficient	5.0×10^{-5}	6.2×10^{-5}	$m^2\,mm^{-3}$
H_I	Half-saturation constant for light	11	14	$\mu mol\ photons\,m^{-2}\,s^{-1}$
$U_{max,CO2}$	Maximum uptake rate of CO2	11.2	8.2	$\mu mol\,mm^{-3}$ per day
H_{CO2}	Half-saturation constant for CO2	2.0	0.5	$\mu mol\,l^{-1}$
r_{max}	Maximum respiration rate	1.0	1.1	$\mu mol\,mm^{-3}$ per day
$U_{max,HCO3}$	Maximum uptake rate of HCO3⁻	9.5	7.3	$\mu mol\,mm^{-3}$ per day
H_{HCO3}	Half-saturation constant for HCO3⁻	200	75	$\mu mol\,l^{-1}$
Q_{min}	Minimum carbon content	15	9	$\mu mol\,mm^{-3}$
Q_{max}	Maximum carbon content	17	17	$\mu mol\,mm^{-3}$
y_N	Cellular N:C ratio	0.14	0.18	Molar
y_P	Cellular P:C ratio	6.0×10^{-3}	8.0×10^{-3}	Molar
y_S	Cellular S:C ratio	5.0×10^{-3}	7.6×10^{-3}	Molar
V	Cell volume	$47–87 \times 10^{-9}$	35×10^{-9}	mm^3 per cell
MC	Cellular microcystin content	0	0.52	$\mu g\,mm^{-3}$
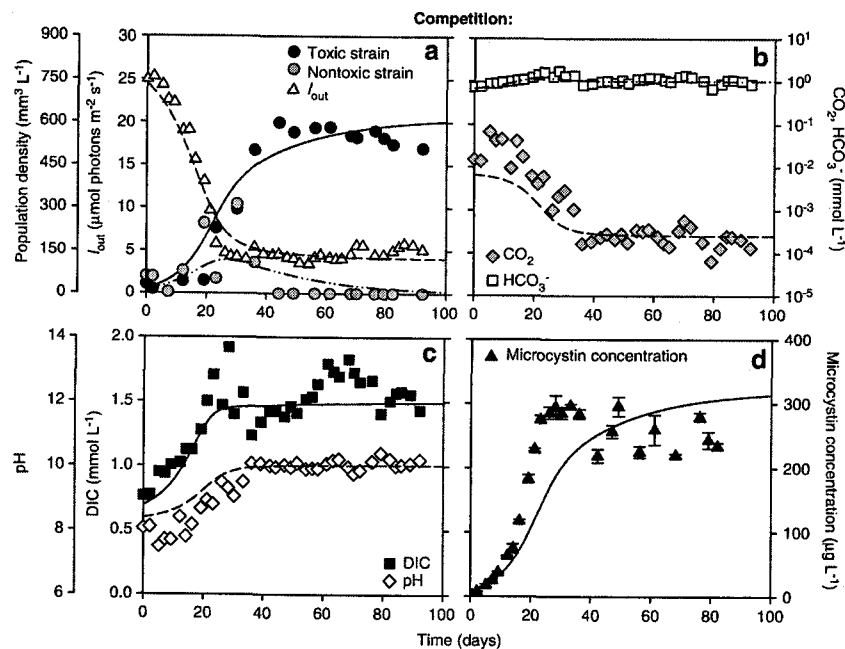
Figure 3 Competition between the toxic and non-toxic strain in a CO₂-limited chemostat. (a) The toxic strain *Microcystis* CYA140 displaces the non-toxic strain *Microcystis* CYA43. I_{out} represents the light intensity penetrating through the chemostat. (b) CO₂ and bicarbonate concentrations. (c) Dissolved inorganic carbon (DIC) and pH. (d) Total microcystin concentration (error bars indicate s.d.). Symbols represent chemostat data, lines show the model predictions. Parameter values are given in Tables 1 and 2.

confirming the competitive dominance of the toxic strain (Figure 3d).

Light-limited experiments

We also tested our model predictions against experiments performed under light-limited but CO₂-replete conditions by Kardinaal *et al.* (2007b). They measured population densities and light availability, but did not measure alkalinity and inorganic carbon. In their monoculture experiments, population densities increased while light penetration

through the chemostats (I_{out}) was reduced to very low values of $\sim 1.3\ \mu mol\ photons\ m^{-2}\ s^{-1}$ (Figures 4a and b). The pH varied between 8.2 and 8.5. This is close to the pH of the mineral medium itself, and far below the pH of 9.8 to 10 measured under carbon-limited conditions (Figures 2e and f). These observations confirm that the experiments were indeed performed under light-limited conditions.

According to our parameter estimates, the non-toxic strain has a slightly lower half-saturation constant for light and higher maximum uptake rates for inorganic carbon than the toxic strain (Table 2).
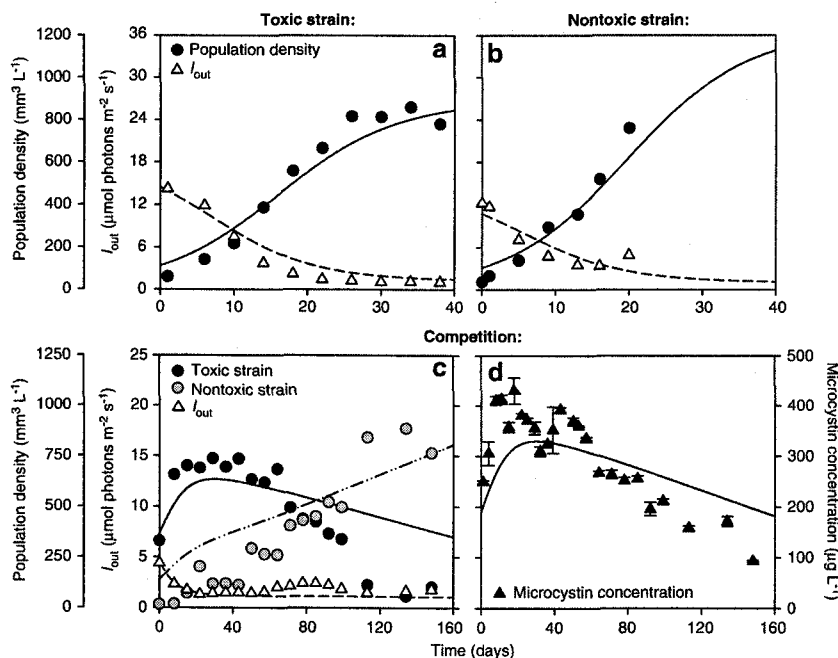
Figure 4 Monoculture and competition experiments between the toxic and non-toxic strain in a light-limited chemostat. (a, b) Population density (expressed as biovolumes) and light intensity penetrating through the chemostat (I_{out}) in monoculture experiments of (a) the toxic strain *Microcystis* CYA140, and (b) the non-toxic strain *Microcystis* CYA43. (c) In competition, the non-toxic strain *Microcystis* CYA43 displaces the toxic strain *Microcystis* CYA140. (d) Total microcystin concentration in the competition experiment (error bars indicate s.d.). Symbols represent chemostat data, lines show the model predictions. Parameter values are given in Tables 1 and 2. The chemostat data in this figure are from Kardinaal *et al.* (2007b).

Hence, the model predicts that the non-toxic strain should be a slightly better competitor for light. This model prediction is confirmed by the competition experiment. Both strains initially increased while light penetration through the chemostat (I_{out}) was reduced (Figure 4c). Subsequently, the toxic strain was slowly replaced by the non-toxic strain during a 160-days period. The total microcystin concentration increased during the first 20 days of the competition experiment and subsequently decreased until the end of the experiment, consistent with the gradual replacement of the toxic by the non-toxic strain (Figure 4d).

In total, the competition experiments show that the toxic strain became dominant under CO_2-limited conditions, whereas the non-toxic strain dominated under high CO_2 but light-limited conditions. The model predictions captured this reversal in competitive dominance, and were largely in agreement with the experiments (Figures 3 and 4).

Discussion

Mechanisms of competition
In this study, we have demonstrated that competition for inorganic carbon can be successfully predicted from a relatively simple model that includes the basics of inorganic carbon chemistry and the key physiological traits of the species involved. An important aspect of competition for

inorganic carbon is the strong interplay between CO_2, bicarbonate and pH in aquatic ecosystems. More specifically, as observed in our experiments, carbon assimilation leads to CO_2 depletion accompanied by an increase in pH, shifting the carbon chemistry toward a predominance of bicarbonate (Figures 1 and 2). This is consistent with field studies of the inorganic carbon chemistry of eutrophic waters, where dense phytoplankton blooms can deplete the CO_2 concentration, thereby inducing high pH values in both freshwater (Talling, 1976; Maberly, 1996) and marine ecosystems (Hansen, 2002).

Our experiments show that the toxic strain was able to reduce the concentration of dissolved CO_2 to a lower level than the non-toxic strain (Figures 2c and d), and won the competition (Figure 3). That is, the winner of competition had the lowest R^* value for CO_2, as in traditional resource competition models (Tilman, 1982). An alternative explanation for our results is that the pH tolerance differed between the strains. Indeed, in monoculture, the toxic strain enhanced pH to higher values than the non-toxic strain (Figures 2e and f). Hence, the outcome of our experiments might also be explained by differences in pH* values. However, pH drift experiments (not shown) indicated that both strains could tolerate high pH up to ~11.2, and that variation in pH had little effect on the specific growth rates of the two strains over the entire pH range covered by our experiments. These findings

1446

are consistent with Bañares-España *et al.* (2006), who showed that the pH tolerance of 19 different *Microcystis* strains ranged from 10.4 to 11.7, that is, they could all tolerate high pH. Therefore, our model assumed that pH does not have a direct effect on the specific growth rates. Yet, although *Microcystis* may tolerate high pH, several studies have shown that pH > 9 often approaches or even exceeds the pH tolerance of other phytoplankton species (Goldman *et al.*, 1982; Hansen, 2002). Further competition experiments with species of different pH sensitivity are therefore recommended to investigate the impact of changes in pH on phytoplankton community composition.

Given the high bicarbonate concentrations, one may question whether CO_2 depletion by cyanobacteria indeed leads to carbon-limited conditions, as many species can utilize bicarbonate as additional carbon source. CO_2 easily diffuses across cell membranes. In contrast, bicarbonate uptake requires active transport mechanisms to cross the cell membrane or the presence of extracellular carbonic anhydrases converting bicarbonate into CO_2 (Kaplan and Reinhold, 1999; Elzenga *et al.*, 2000; Badger *et al.*, 2006). Hence, phytoplankton species typically have a much lower affinity for bicarbonate than for CO_2 (for example, Rost *et al.*, 2003; Kranz *et al.*, 2009). This is consistent with our study, where we estimated that the half-saturation constant for bicarbonate was more than two orders of magnitude higher than the half-saturation constant for CO_2 (Table 2). This implies that cells strongly rely on CO_2 as their preferred carbon source. For instance, our model estimates that 50–55% of the total carbon uptake during the first days of the competition experiment was attributed to CO_2, even though CO_2 concentrations were much lower than bicarbonate concentrations (Figure 3). When CO_2 was depleted and bicarbonate concentrations increased during the course of the competition experiment, the contribution of CO_2 to the total carbon uptake became lower but still amounted to 29% for the toxic strain and 14% for the non-toxic strain. Similar percentages have been reported for other phytoplankton species (for example, Rost *et al.*, 2003). Thus, the carbon source for phytoplankton growth gradually shifted from combined CO_2 and bicarbonate uptake to predominantly bicarbonate uptake. According to our model simulations, the low uptake rate of bicarbonate was insufficient to sustain high growth rates of the *Microcystis* strains, such that their growth rates became carbon limited when CO_2 was depleted.

An increase in CO_2 supply and reduction of the incident light intensity shifted our experiments from competition for inorganic carbon to competition for light. This transition caused a reversal in competitive dominance. The strain dominating under carbon-limited conditions lost the competition under light-limited conditions. This finding might be highly relevant. If the reversal in competitive

dominance is not restricted to our particular study system but widespread in natural communities, the current rise in atmospheric CO_2 levels may cause major changes in the species composition of algal blooms, from superior carbon competitors to superior light competitors.

The role of microcystins in competition

Harmful cyanobacteria may form dense blooms in eutrophic waters (Reynolds, 1987; Paerl and Huisman, 2008), and can produce a variety of toxins including microcystins that pose a major threat to birds, mammals and human health (Chorus and Bartram, 1999; Carmichael, 2001; Huisman *et al.*, 2005). Interestingly, cyanobacterial blooms often consist of mixtures of toxic and non-toxic strains (Kurmayer and Kutzenberger, 2003; Kardinaal *et al.*, 2007a; Briand *et al.*, 2008; Briand *et al.*, 2009). In our experiments, the toxic strain was the better competitor for inorganic carbon, whereas the non-toxic strain was the better competitor for light. As these results rely on one toxic and one non-toxic strain only, the observed association between toxin production and competitive ability might be mere coincidence.

However, Jähnichen *et al.* (2001) hypothesized earlier that microcystins might have a possible function in carbon assimilation at low CO_2 availability. Specifically, by drawing an analogy with okadaic acid, they argued that microcystins might suppress carbon losses due to photorespiration by the RuBisCO enzyme. Consistent with this hypothesis, immunogold localization pointed at relatively high densities of microcystin within carboxysomes (Gerbersdorf, 2006), which are intracellular microcompartments containing high RuBisCO concentrations to facilitate the carbon-concentrating mechanism of cyanobacteria (for example, Badger *et al.*, 2006; Price *et al.*, 2008). However, Young *et al.* (2005, 2008) did not confirm preferential localization of microcystins within carboxysomes, and found instead that microcystins were mainly associated with the thylakoids and polyphosphate bodies. Jähnichen *et al.* (2007) provided some indirect support for their hypothesis that microcystins are involved in carbon assimilation using a series of ingenious experiments in which they restricted sodium-dependent bicarbonate uptake through replacement of sodium by potassium in the growth medium. Yet, none of these data provide conclusive evidence that microcystin production indeed confers a selective advantage under carbon-limited conditions.

Therefore, we ran additional competition experiments with the microcystin-producing strain *M. aeruginosa* PCC 7806 and its *mcyB* mutant. This mutant, which does not produce microcystins, was generated by insertion of a chloramphenicol resistance cassette into the *mcyB* gene (Dittmann *et al.*, 1997). We quantified population densities of the
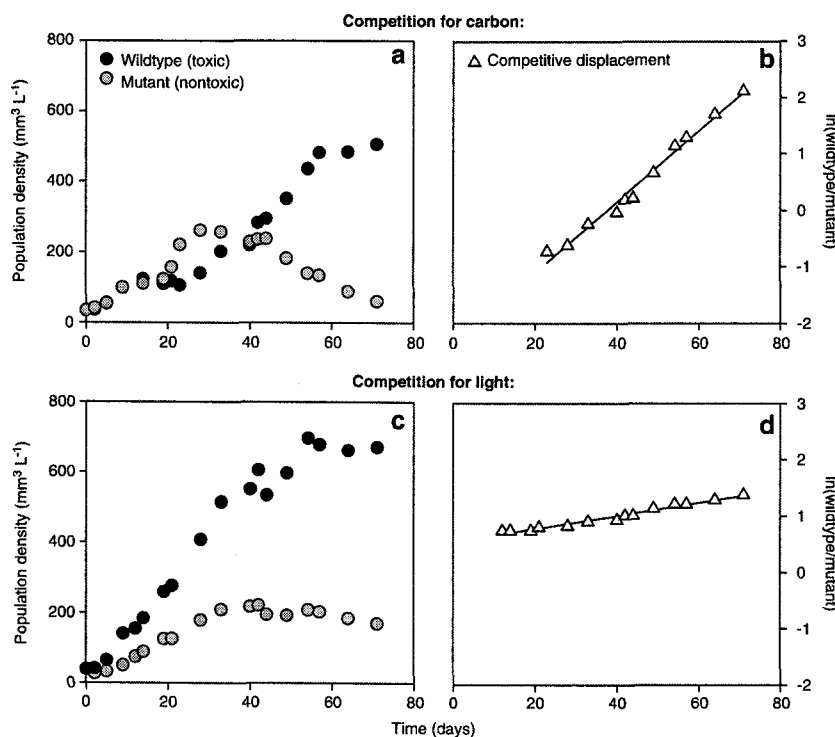
Figure 5 Competition experiments between the wild type strain *M. aeruginosa* PCC 7806 and its *mcyB* mutant. (**a, b**) Competition in a CO₂-limited chemostat. (**c, d**) Competition in a light-limited chemostat. The rate of competitive displacement (RCD) is estimated from the slope of the linear regression of ln(wild type/mutant) versus time. Comparison of the slopes in (**b**) and (**d**) shows that the wild type displaces the mutant at a much faster rate in the CO₂-limited chemostat (RCD = 0.063 per day) than in the light-limited chemostat (RCD = 0.012 per day). Regression statistics: (**b**) $y = 0.063x - 2.371$ ($R^2 = 0.98$; $P < 0.001$); (**d**) $y = 0.012x + 0.518$ ($R^2 = 0.96$; $P < 0.001$).

wild type and mutant during the competition experiments using qPCR targeted at the chloramphenicol resistance cassette of the mutant. For this purpose, we developed two new primers (Maeru-CmF: 5'-TT CGAATTTCTGCCATTCAT-3' and Maeru-CmR: 5'-ATT ATACGCAAGGCGACAAG-3'). The competition experiments were performed using exactly the same conditions as in our other experiments. Under carbon-limited conditions, the wild type displaced the mutant (Figure 5a). Under light-limited conditions, the wild type and mutant coexisted for the entire duration of the experiment, although the wild type was dominant and the mutant slowly declined from day 40 onwards (Figure 5c). To assess the selective advantage of the microcystin-producing wild type, we calculated the rate of competitive displacement (RCD; Grover, 1991b; Passarge *et al.*, 2006). The RCD can be interpreted as the difference in fitness between the wild type and its mutant. Specific growth rates (μ) of the wild type (WT) and mutant (M) are defined as:

$$\mu_{WT} = \frac{1}{X_{WT}} \frac{dX_{WT}}{dt}$$

and

$$\mu_M = \frac{1}{X_M} \frac{dX_M}{dt} \qquad (5)$$

As the time derivative of ln(X) equals $(1/X)(dX/dt)$, the RCD is given by:

$$RCD = \mu_{WT} - \mu_M = \frac{d\ln(X_{WT}/X_M)}{dt} \qquad (6)$$

Hence, the RCD can be estimated as the slope of the linear regression of ln(wild type/mutant) versus time. The RCD estimates confirm that the wild type displaced the mutant at a much faster rate under carbon-limited conditions (Figure 5b; RCD = 0.063 per day) than under light-limited conditions (Figure 5d; RCD = 0.012 per day). This direct comparison between a microcystin-producing wild type and its mutant demonstrates that microcystin production confers a strong selective advantage under carbon-limited conditions, whereas this selective advantage largely disappears when CO₂ is in ample supply.

Kardinaal *et al.* (2007b) hypothesized that non-toxic strains are generally better competitors for light, because the energy required for microcystin production is less available under light-limited conditions. However, this hypothesis is not supported by our experiments, as the mutant did not replace the wild type under light-limited conditions (Figures 5c and d). There are several possible explanations for this discrepancy. For instance, energetic costs of microcystin production might be

1448

relatively low, as microcystin represents only a minor fraction of the total cellular carbon and nitrogen budgets (Van de Waal et al., 2009). This line of arguments would explain the very slow competitive displacement of toxic strain CYA140 by non-toxic strain CYA43 (Figure 4), and the nearly neutral coexistence of wild type strain PCC 7806 and its mutant under light-limited conditions (Figures 5c and d). Alternatively, it might be that the mutant strain still carries some of the costs associated with microcystin production. Although this mutant cannot produce microcystin because its mcyB gene is disrupted, transcript analyses have shown that transcription of its mcyABC operon remains unaffected (Tillett et al., 2000). Accordingly, even though the hypothesis of Kardinaal et al. (2007b) does not apply to this specific mutant, it might still apply to other non-toxic strains lacking the entire mcy gene cluster. More strains need to be investigated before the hypothesis of Kardinaal et al. (2007b) can be fully evaluated.

In conclusion, our results provide a first step towards a better understanding of competition for inorganic carbon among cyanobacteria. We have shown that microcystin production provides a selective advantage under carbon-limited conditions. In addition, we have demonstrated that rising CO_2 availability can lead to a reversal in the outcome of competition between a toxic and non-toxic strain. However, our work also raises new questions for future research. For instance, what is the role of pH tolerance in competition for inorganic carbon? And what is the underlying molecular mechanism for the observed selective advantage of microcystin production?

Acknowledgements

References

Badger MR, Price GD, Long BM, Woodger FJ. (2006). The environmental plasticity and ecological genomics of the cyanobacterial CO_2 concentrating mechanism. J Exp Bot 57: 249–265.

Bañares-España E, López-Rodas V, Salgado C, Costas E, Flores-Moya A. (2006). Inter-strain variability in the photosynthetic use of inorganic carbon, exemplified by the pH compensation point, in the cyanobacterium Microcystis aeruginosa. Aquat Bot 85: 159–162.

Behrenfeld MJ, O'Malley RT, Siegel DA, McClain CR, Sarmiento JL, Feldman GC et al. (2006). Climate-driven trends in contemporary ocean productivity. Nature 444: 752–755.

Briand E, Gugger M, François JC, Bernard C, Humbert JF, Quiblier C. (2008). Temporal variations in the dynamics of potentially microcystin-producing strains in a bloom-forming Planktothrix agardhii (Cyanobacterium) population. Appl Environ Microb 74: 3839–3848.

Briand E, Escoffier N, Straub C, Sabart M, Quiblier C, Humbert JF. (2009). Spatiotemporal changes in the genetic diversity of a bloom-forming Microcystis aeruginosa (cyanobacteria) population. ISME J 3: 419–429.

Caraco NF, Miller R. (1998). Effects of CO_2 on competition between a cyanobacterium and eukaryotic phytoplankton. Can J Fish Aquat Sci 55: 54–62.

Carmichael WW. (2001). Health effects of toxin-producing cyanobacteria: 'the cyanoHABs'. Hum Ecol Risk Assess 7: 1393–1407.

Chen YW, Qin BQ, Teubner K, Dokulil MT. (2003). Long-term dynamics of phytoplankton assemblages: Microcystis-domination in Lake Taihu, a large shallow lake in China. J Plankton Res 25: 445–453.

Chorus I, Bartram J. (1999). Toxic Cyanobacteria in Water: A Guide to their Public Health Consequences, Monitoring and Management. E&FN Spon: London.

Dittmann E, Neilan BA, Erhard M, von Döhren H, Börner T. (1997). Insertional mutagenesis of a peptide synthetase gene that is responsible for hepatotoxin production in the cyanobacterium Microcystis aeruginosa PCC 7806. Mol Microbiol 26: 779–787.

Doblin MA, Coyne KJ, Rinta-Kanto JM, Wilhelm SW, Dobbs FC. (2007). Dynamics and short-term survival of toxic cyanobacteria species in ballast water from NOBOB vessels transiting the Great Lakes: implications for HAB invasions. Harmful Algae 6: 519–530.

Doney SC, Fabry VJ, Feely RA, Kleypas JA. (2009). Ocean acidification: the other CO_2 problem. Annu Rev Mar Sci 1: 169–192.

Droop MR. (1973). Some thoughts on nutrient limitation in algae. J Phycol 9: 264–272.

Ducobu H, Huisman J, Jonker RR, Mur LR. (1998). Competition between a prochlorophyte and a cyanobacterium under various phosphorus regimes: comparison with the Droop model. J Phycol 34: 467–476.

Elzenga JTM, Prins HBA, Stefels J. (2000). The role of extracellular carbonic anhydrase activity in inorganic carbon utilization of Phaeocystis globosa (Prymnesiophyceae): a comparison with other marine algae using the isotopic disequilibrium technique. Limnol Oceanogr 45: 372–380.

Fastner J, Flieger I, Neumann U. (1998). Optimised extraction of microcystins from field samples: a comparison of different solvents and procedures. Water Res 32: 3177–3181.

Field CB, Behrenfeld MJ, Randerson JT, Falkowski P. (1998). Primary production of the biosphere: integrating terrestrial and oceanic components. Science 281: 237–240.

Gerbersdorf SU. (2006). An advanced technique for immuno-labelling of microcystins in cryosectioned cells of Microcystis aeruginosa PCC 7806 (cyanobacteria): implementation of an experiment with varying light scenarios and culture densities. Toxicon 47: 218–228.

Goldman JC, Riley CB, Dennett MR. (1982). The effect of pH in intensive microalgal cultures. II. Species competition. J Exp Mar Biol Ecol 57: 15–24.

Grover JP. (1991a). Resource competition in a variable environment: phytoplankton growing according to the variable-internal-stores model. *Am Nat* **138**: 811–835.

Grover JP. (1991b). Resource competition among microalgae in variable environments: experimental tests of alternative models. *Oikos* **62**: 231–243.

Grover JP. (1997). *Resource Competition*. Chapman & Hall: London.

Hansen PJ. (2002). Effect of high pH on the growth and survival of marine phytoplankton: implications for species succession. *Aquat Microb Ecol* **28**: 279–288.

Hein M. (1997). Inorganic carbon limitation of photosynthesis in lake phytoplankton. *Freshwater Biol* **37**: 545–552.

Huisman J, Jonker RR, Zonneveld C, Weissing FJ. (1999). Competition for light between phytoplankton species: experimental tests of mechanistic theory. *Ecology* **80**: 211–222.

Huisman J, Matthijs HCP, Visser PM (eds) (2005). *Harmful Cyanobacteria*. Springer: Berlin.

Huisman J, Sharples J, Stroom JM, Visser PM, Kardinaal WEA, Verspagen JMH et al. (2004). Changes in turbulent mixing shift competition for light between phytoplankton species. *Ecology* **85**: 2960–2970.

Ibelings BW, Maberly SC. (1998). Photoinhibition and the availability of inorganic carbon restrict photosynthesis by surface blooms of cyanobacteria. *Limnol Oceanogr* **43**: 408–419.

Jähnichen S, Ihle T, Petzoldt T, Benndorf J. (2007). Impact of inorganic carbon availability on microcystin production by *Microcystis aeruginosa* PCC 7806. *Appl Environ Microb* **73**: 6994–7002.

Jähnichen S, Petzoldt T, Benndorf J. (2001). Evidence for control of microcystin dynamics in Bautzen reservoir (Germany) by cyanobacterial population growth rates and dissolved inorganic carbon. *Arch Hydrobiol* **150**: 177–196.

Johnson KJ. (1982). Carbon dioxide hydration and dehydration kinetics in seawater. *Limnol Oceanogr* **27**: 849–855.

Kaplan A, Reinhold L. (1999). CO₂ concentrating mechanisms in photosynthetic microorganisms. *Annu Rev Plant Physiol Plant Mol Biol* **50**: 539–570.

Kardinaal WEA, Janse I, Kamst-Van Agterveld M, Meima M, Snoek J, Mur LR et al. (2007a). *Microcystis* genotype succession in relation to microcystin concentrations in freshwater lakes. *Aquat Microb Ecol* **48**: 1–12.

Kardinaal WEA, Tonk L, Janse I, Hol S, Slot P, Huisman J et al. (2007b). Competition for light between toxic and nontoxic strains of the harmful cyanobacterium *Microcystis*. *Appl Environ Microbiol* **73**: 2939–2946.

Klausmeier CA, Litchman E, Daufresne T, Levin SA. (2004). Optimal nitrogen-to-phosphorus stoichiometry of phytoplankton. *Nature* **429**: 171–174.

Kranz SA, Sültemeyer D, Richter KU, Rost B. (2009). Carbon acquisition by *Trichodesmium*: the effect of pCO2 and diurnal changes. *Limnol Oceanogr* **54**: 548–599.

Kurmayer R, Kutzenberger T. (2003). Application of real-time PCR for quantification of microcystin genotypes in a population of the toxic cyanobacterium *Microcystis* sp. *Appl Environ Microbiol* **69**: 6723–6730.

Lawton LA, Edwards C, Codd GA. (1994). Extraction and high-performance liquid chromatographic method for the determination of microcystins in raw and treated waters. *Analyst* **119**: 1525–1530.

Litchman E, Klausmeier CA. (2001). Competition of phytoplankton under fluctuating light. *Am Nat* **157**: 170–187.

Maberly SC. (1996). Diel, episodic and seasonal changes in pH and concentrations of inorganic carbon in a productive lake. *Freshwater Biol* **35**: 579–598.

Maberly SC, Ball LA, Raven JA, Sültemeyer D. (2009). Inorganic carbon acquisition by chrysophytes. *J Phycol* **45**: 1052–1061.

Martin CL, Tortell PD. (2008). Bicarbonate transport and extracellular carbonic anhydrase in marine diatoms. *Physiol Plantarum* **133**: 106–116.

Morel FMM. (1987). Kinetics of nutrient uptake and growth in phytoplankton. *J Phycol* **23**: 137–150.

Murphy J, Riley JP. (1962). A modified single-solution method for the determination of phosphate in natural waters. *Water Sci Technol* **32**: 25–34.

Orr JC, Fabry VJ, Aumont O, Bopp L, Doney SC, Feely RA et al. (2005). Anthropogenic ocean acidification over the twenty-first century and its impact on calcifying organisms. *Nature* **437**: 681–686.

Paerl HW, Huisman J. (2008). Blooms like it hot. *Science* **320**: 57–58.

Passarge J, Hol S, Escher M, Huisman J. (2006). Competition for nutrients and light: stable coexistence, alternative stable states, or competitive exclusion? *Ecol Monogr* **76**: 57–72.

Price GD, Badger MR, Woodger FJ, Long BM. (2008). Advances in understanding the cyanobacterial CO₂-concentrating-mechanism (CCM): functional components, Ci transporters, diversity, genetic regulation and prospects for engineering into plants. *J Exp Bot* **59**: 1441–1461.

Rantala A, Fewer DP, Hisbergues M, Rouhiainen L, Vaitomaa J, Börner T et al. (2004). Phylogenetic evidence for the early evolution of microcystin synthesis. *Proc Natl Acad Sci USA* **101**: 568–573.

Raven JA. (1991). Implications of inorganic carbon utilization: ecology, evolution, and geochemistry. *Can J Bot* **69**: 908–924.

Reynolds CS. (1987). Cyanobacterial water blooms. *Adv Bot Res* **13**: 67–143.

Riebesell U, Schulz KG, Bellerby RGJ, Botros M, Fritsche P, Meyerhöfer M et al. (2007). Enhanced biological carbon consumption in a high CO₂ ocean. *Nature* **450**: 545–549.

Rinta-Kanto JM, Ouellette AJA, Boyer GL, Twiss MR, Bridgeman TB, Wilhelm SW. (2005). Quantification of toxic *Microcystis* spp. during the 2003 and 2004 blooms in western Lake Erie using quantitative real-time PCR. *Environ Sci Technol* **39**: 4198–4205.

Rost B, Riebesell U, Burkhardt S, Sültemeyer D. (2003). Carbon acquisition of bloom-forming marine phytoplankton. *Limnol Oceanogr* **48**: 55–67.

Rost B, Zondervan I, Wolf-Gladrow D. (2008). Sensitivity of phytoplankton to future changes in ocean carbonate chemistry: current knowledge, contradictions and research directions. *Mar Ecol Prog Ser* **373**: 227–237.

Solomon S, Qin D, Manning M, Marquis M, Averyt K, Tignor MMB et al. (2007). *Climate Change 2007: The Physical Science Basis. Contribution of Working Group I to the Fourth Assessment Report of the Intergovernmental Panel on Climate Change*. Cambridge University Press: Cambridge.

Sommer U. (1985). Comparison between steady state and non-steady state competition: experiments with natural phytoplankton. *Limnol Oceanogr* **30**: 335–346.

1450

Stomp M, Huisman J, De Jongh F, Veraart AJ, Gerla D, Rijkeboer M et al. (2004). Adaptive divergence in pigment composition promotes phytoplankton biodiversity. Nature 432: 104–107.

Stumm W, Morgan JJ. (1996). Aquatic Chemistry: Chemical Equilibria and Rates in Natural Waters. Wiley-Interscience: New York.

Talling JF. (1976). The depletion of carbon dioxide from lake water by phytoplankton. J Ecol 64: 79–121.

Tillett D, Dittmann E, Erhard M, von Döhren H, Börner T, Neilan BA. (2000). Structural organization of microcystin biosynthesis in Microcystis aeruginosa PCC7806: an integrated peptide-polyketide synthetase system. Chem Biol 7: 753–764.

Tilman D. (1982). Resource Competition and Community Structure. Princeton University Press: Princeton.

Tonk L, Visser PM, Christiansen G, Dittmann E, Snelder EOFM, Wiedner C et al. (2005). The microcystin composition of the cyanobacterium Planktothrix agardhii changes towards a more toxic variant with increasing light intensity. Appl Environ Microbiol 71: 5177–5181.

Tortell PD, DiTullio GR, Sigman DM, Morel FMM. (2002). CO$_2$ effects on taxonomic composition and nutrient utilization in an Equatorial Pacific phytoplankton assemblage. Mar Ecol Prog Ser 236: 37–43.

Vaitomaa J, Rantala A, Halinen K, Rouhiainen L, Tallberg P, Mokelke L et al. (2003). Quantitative real-time PCR for determination of microcystin synthetase E copy numbers for Microcystis and Anabaena in lakes. Appl Environ Microb 69: 7289–7297.

Van de Waal DB, Verspagen JMH, Lürling M, Van Donk E, Visser PM, Huisman J. (2009). The ecological stoichiometry of toxins produced by harmful cyanobacteria: an experimental test of the carbon-nutrient balance hypothesis. Ecol Lett 12: 1326–1335.

Van der Grinten E, Lürling M, Burger-Wiersma T. (2000). Is Microcystis really toxic to Daphnia? Verh Internat Verein Limnol 27: 3226–3229.

Verspagen JMH, Passarge J, Jöhnk KD, Visser PM, Peperzak L, Boers P et al. (2006). Water management strategies against toxic Microcystis blooms in the Dutch delta. Ecol Appl 16: 313–327.

Wetzel RG, Likens GE. (2000). Limnological Analyses, 3rd edn Springer-Verlag: New York.

Williams TG, Turpin DH. (1987). Photosynthetic kinetics determine the outcome of competition for dissolved inorganic carbon by freshwater microalgae: implications for acidified lakes. Oecologia 73: 307–311.

Young FM, Morrison LF, James J, Codd GA. (2008). Quantification and localization of microcystins in colonies of a laboratory strain of Microcystis (Cyanobacteria) using immunological methods. Eur J Phycol 43: 217–225.

Young FM, Thomson C, Metcalf JS, Lucocq JM, Codd GA. (2005). Immunogold localisation of microcystins in cryosectioned cells of Microcystis. J Struct Biol 151: 208–214.

Supplementary Information accompanies the paper on The ISME Journal website (http://www.nature.com/ismej)